Cosmic Ray and Laser Simulations for the STAR TPC

Peter G. Jones

School of Physics and Astronomy
University of Birmingham
Edgbaston
Birmingham, B15 2TT, U.K.

July 2, 1997

Abstract

This note summarizes the status of cosmic ray and laser simulations for the tests of the STAR TPC. The results contained are based in part on parametrizations of the TPC response built into the TPC fast simulator and assume ideal tracking. Three possible distortions have been studied: a shorted stripe on the outer fieldcage; a mismatch of the potential on the pad plane with that of the field cages and a mismatch of the HV potential. Simulations were performed to detect a 700 μm maximum radial distortion. Consideration has been given to the required statistical accuracy needed to identify this level of distortion.

1 Introduction

The aim of the cosmic ray simulations was to determine an analysis strategy for identifying electric field distortions caused by defects in the outer field cage or misplacement of potential surfaces with respect to the inner and outer field cages. Electrostatic calculations [1] have shown that two types of defect my give rise to distortions which exceed a 700 μm maximum radial distortion. These are a shorted stripe (a short between two of the equipotential rings which comprise the outer and inner field cages) and a misplacement of the pad plane or HV membrane (so-called plunger effect). Of the two types of distortion the plunger effects are the most subtle, the degree of distortion depending on the potential mismatch due to misplacement of the potential surface with respect to that on the inner and outer field cages. Whilst the effect at the pad plane can be corrected by changing the bias on the gating grid, there is no such mechanism for changing the bias on the HV membrane.

In order to correctly simulate the various types of distortion a new analysis module has been written which calculates the radial distortion integral [1] on a point-by-point basis. Due to the cylindrical symmetry of the STAR TPC, the distortion azimuthally symmetric for each of the possible defects considered here, whilst the magnitude of the distortion is a function of both radius and position in the drift direction. Straight tracks, either cosmic ray muons or laser tracks are distorted in the presence of such defects. It is the shape of this distortion and its drift length dependence which make it possible to differentiate between the different types of defect which may be present.

One final consideration is that since the distortion is radial, then a track which is directed along a radial line will not appear distorted. Deviation from straightness is larger for larger crossing angles, but here is the rub: the position resolution is also a function of crossing angle. Preliminary calculations [2] have indicated that the optimal crossing angle is around 25 degrees.

2 Cosmic Ray and Laser Event Generators

Cosmic ray muons were generated using the HemiCosm generator, originally written by Michael Paul Bringle for the BaBar experiment [3]. Douglas Greiner wrote the STAR version of the main program which outputs `tx` format input for GSTAR. The author modified this program to simulate different trigger conditions. The event rates quoted in this note are taken from the output of HemiCosm. Laser tracks were generated using a program written by Ken Barish, which he kindly made available. The laser system geometry is described elsewhere [4].

3 Geometry

Eight Central Trigger Barrel (CTB) trays will be available for triggering on cosmic ray muons for the TPC system test. These have to be arranged in such a way as to provide tracks with the appropriate crossing angle. Enough Front End Electronics (FEE) cards will be available to arm one supersector. For ease of access, sectors 6 and 18 (6 o'clock position) will be used in the test. A laser raft is also available in these sectors.

In order to sufficiently narrow the angular acceptance of tracks in the simulations a single CTB tray was located in position 27 [5], below sector 6. Five CTB trays located in positions 47–51, above sectors 10 and 11, give average crossing angles between 24–36 degrees in sector 6. In this geometry almost all tracks have full coverage in the outer sector, and very little coverage in the inner sector. The remaining CTB slats could be used to locate tracks which cross the inner sector, but this has not been studied in detail. The problem with the inner sector is that the pad rows are widely spaced and large crossing angles mean that tracks tend to leave few hits. For this reason, only the outer sector has been used in this study.

With this geometry HemiCosm predicts a trigger rate of 0.78 Hz for cosmic ray muons in the momentum range 1–1000 GeV/c, for 1 scintillator in each tray (*i.e.* one half of the total drift length). The incident flux on the upper 5 scintillators varies between 15–23 Hz between positions 47–51. This corresponds to a single scintillator coincidence rate between 1 event every 7.8 seconds and 1 event every 5.5 seconds. This rate is close to the expected maximum MiniDAQ rate. In tests, the coincidence rate was found to be somewhat higher than the HemiCosm prediction.

Another consideration in choosing the position of the lower CTB scintillator is that the outer padrow is closest to the outer field cage at the edge of the row (since the pad rows are straight and are therefore not at a constant radius). However, here a radial line makes a 15 degree angle with respect to the pads. This means that no distortion would be seen for tracks incident with a 15 degree crossing angle. By contrast, in the centre of the pad row, the radial line is perpendicular to the row and a 15 degree crossing angle track here would appear distorted. The chosen position of the bottom scintillator is between these two extremes, being in the intermediate position.

4 Analysis

The HemiCosm generator was used to produce ten thousand triggered cosmic ray events, satisfying the selection criterion of a CTB hit in one of slats 47–51 and a hit in slat 27. HemiCosm predicts the incident muon flux on the surface of a cylinder (the STAR TPC), and the exit point was simply calculated by geometry. The events, covering approximately one half of the total drift length (z=0–110 cm), were processed by GSTAR/G2T using the appropriate detector geometry files. The output of G2T was then subject to the distortion package (`tdi_rdi`) which added one of four possible distortions to the data. A control sample of events, to which no distortion was added constituted a fifth data set. The radial and z position dependences of the various distortions are shown in Figure 1.

The TPC response was simulated by the Tpc Fast Simulator (TFS), where the resolution parameters had been tuned to match Roy Bossingham's standalone simulation of the TPC hit finder using a weighted mean algorithm [6]. The events were reconstructed using the `tte_track` module in the Tpc Track Evaluation package. The results shown in the following sections therefore reflect an ideal case and should be verified using the slow simulator, cluster/hit finder and straight tracker before data taking commences.

4.1 Residual Distributions from Cosmic Ray Tracks

The principal strategy for measuring any distortion is by looking at the deviation of tracks from a straight line, by plotting the residual distribution of hits relative to a straight line fit to some or all the hits found on a track. It turns out that this strategy is not sensitive to a global rotation of a track, since what is measured is the deviation from the average track position. This greatly reduces the observable effect.

4.1.1 Shorted Stripe

The largest effect is caused by a shorted stripe. This has a marked effect on the drift of charge throughout the drift volume, although the largest effects are seen at the location of the short itself. In the simulation, a shorted stripe defect was introduced at $z = 52$ cm. Figure 2, shows the radial distortion as a function of radius at $z = 50$ cm, close to the defect in the outer field cage. Although the maximum distortion is almost 1 cm at the outer row, a fit to all the points in the outer sector would greatly reduce the observable effect. In this case the maximum residual would be less than 1 mm, but this is still a large effect. In order to maximize the observable effect only rows 14–30 in the outer sector were included in the straight line fit. This should lead to a maximum radial distortion of 2.75 mm at the outer row, which corresponds to a 1.1 mm xy residual, taking into account the average crossing angle and the CTB angle with respect to the pad row. Figure 3 shows the residual in the xy and yz planes as a function of TPC pad row number, and the xy residual of the last point as a function of TPC pad row. The first two profile histograms include all the generated tracks. The fact that a distortion is visible at all in the xy residual distribution as function of pad row, shows that all tracks are distorted to a greater or lesser extent. The bottom plot shows the very clear z dependence of the distortion which characterizes the shorted stripe defect.

4.1.2 Plunger Effects

By far the most challenging distortions to detect are the plunger effects caused by misplacement of the pad plane or the HV membrane. As can be seen in Figure 1, a misplacement of the pad plane affects the entire drift volume, whereas a misplacement of the HV membrane affects only charge drifting from within 10-20 cm. In this case, the size of the effect depends on the potential mismatch between either surface and the outer and inner field cages. In the simulation, the potential mismatch has been tuned to $\Delta V/V = 2.5 \times 10^{-4}$, which is equivalent to a 500 μm displacement of either surface and yields a 700 μm maximum radial distortion at the outermost pad row.

Figure 4, shows the radial distortion as a function of radius at $z = 0$ cm. The effect is maximum here for both pad plane and HV membrane plunger effects, although the distortion is oppositely signed. Once again it can be seen that there is a global rotation of the track. Fitting the hits on the inner 17 rows only (the linear part of the curve) the maximum radial distortion would be approximately 225 μm at the outermost pad row. Taking into account the track crossing angle and the angle of the CTB slat leads to an expected shift in the residual distribution of about 85 μm. The mean residual as a function of row and the xy residual of the last row as a function of z position is shown in Figure 5. Since all tracks are equally distorted the average xy residual as a function of row clearly shows a shift of about 70 μm. There is no clear effect in either the yz residual (the other projection) or in the z dependence of the xy residual.

The same set of plots for the HV plunger effect is shown in Figure 6. In this case the effect is prevalent only in the vicinity of the HV membrane. There is no clear effect in the average residuals as function of row, or in the z dependence of the xy residual at the last row. However, the magnitude of the distortion is equal to that observed in the pad plane plunger effects. It is therefore safe to say that the HV plunger effect could be resolved with sufficient statistics localizing tracks close to the HV membrane.

4.1.3 Comment on Statistics

The error on the mean residual, $\sigma_{\overline{xy}}$, is related to the width of the residual distribution, σ_{xy} by the expression,

$$\sigma_{\overline{xy}} = \frac{\sigma_{xy}}{\sqrt{N}} \tag{1}$$

where N is the number of tracks. In this case the width of the residual distribution is approximately 0.2 cm, which means for a sample of 10^4 tracks, the expected error on the mean is 20 μm. Thus a 70 μm effect represents a 3 sigma deviation at this level of statistics.

4.2 Angular Distribution of Laser Tracks

An alternative method that may be employed to study the plunger effects is measuring the angular distribution of laser tracks. In principle, the angle between any two laser beams is known, so by comparing the measured angle with the expected angle gives information about the rotation of any pair of tracks. Since this time it is the rotation of the tracks we wish to measure, all available hits are included in the fit. Another complication is that two bundles of mirrors comprise a single raft, so that even number bundles have one angular separation and odd number bundles another. In this simulation laser tracks from mirrors 3 and 5 were used in the analysis. The relative angle between these tracks is 31 degrees and 36 degrees for odd/even bundles respectively. A sample of 500 laser events were generated, where all mirrors on a single raft were illuminated[1]. Figure 7 shows the angular separation between this pair of laser tracks as a function of the z position of the bundle, for both the pad plane and HV plunger effects. In order to make a comparison between all bundles, it is the difference between the measured and expected angles that is plotted. A clear z dependence in the angular separation is observed, which is expected from Figure 1. The maximum angular difference is about $\frac{1}{50}$ of a degree. This analysis therefore presupposes that the track angle is known to better than $\frac{1}{50}$ of a degree.

5 Conclusion

This study has shown that it is possible to use the residual distributions resulting from a straight line fit to cosmic ray tracks to tell about the possible drift field distortions arising from defects in the outer or inner field cages; or misplacement of the pad plane or HV membrane. It has been demonstrated that radial distortions as small as 700 μm can be observed in the xy residual distributions for a sample of 10^4 cosmic ray tracks in the field distorted region. This result depends in part on the resolution of the TPC reproduced by TFS. If the space point resolution is considerably worse than assumed in this report, then equation 1 can be used to calculate the required statistics, assuming that to first order, the size of the measurable effect does not change with decreased resolution.

A study of the angular distribution of laser tracks has indicated that it is possible in principle to differentiate between pad plane and HV plunger effects, although it has yet to be seen whether the required tolerance of the laser track opening angles can be met.

[1] A technical point concerning this simulation is that due to a problem with GSTAR/G2T at the time the simulation was carried out, *laserinos* were not used. Instead, 10 GeV muons were generated at the appropriate angles and all physics switches (other than energy loss) were turned off in GEANT

References

[1] H.W. Wieman, STAR Note # 253.

[2] M. Lisa, private communication.

[3] M.P. Bringle, BaBar Note # 163.

[4] A. Lebedev, STAR Note in preparation.

[5] H. Matis et. al., STAR Note # 229.

[6] R. Bossingham, STAR Note # 247.

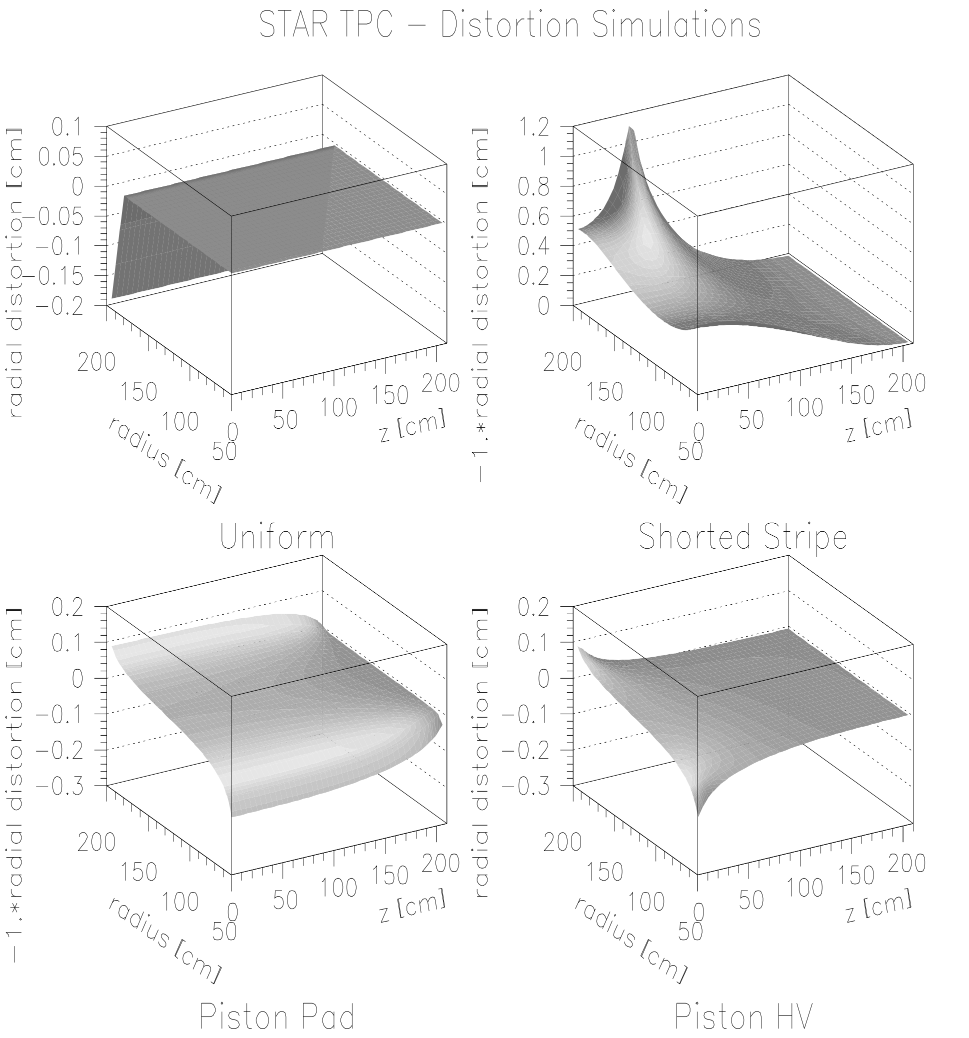

Figure 1: The four types of distortion reproduced by the **tdi** package. The uniform option adds a z independent radial distortion, useful for testing. The other three options reproduce the electric field distortions due a shorted stripe located at $z = 52$ cm, the pad plane plunger effect and the HV plunger effect.

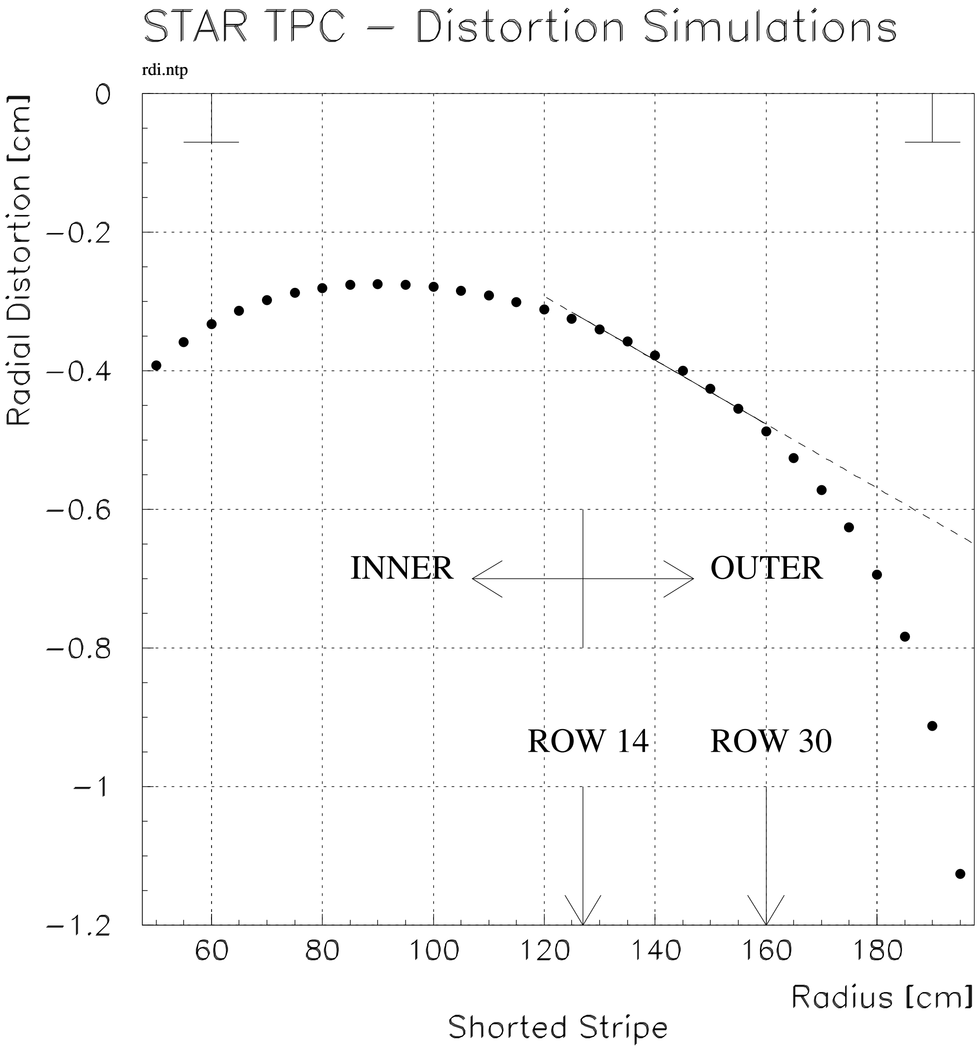

Figure 2: The radial distortion as a function of radius at $z = 50$ cm, for a shorted stripe at $z = 52$ cm.

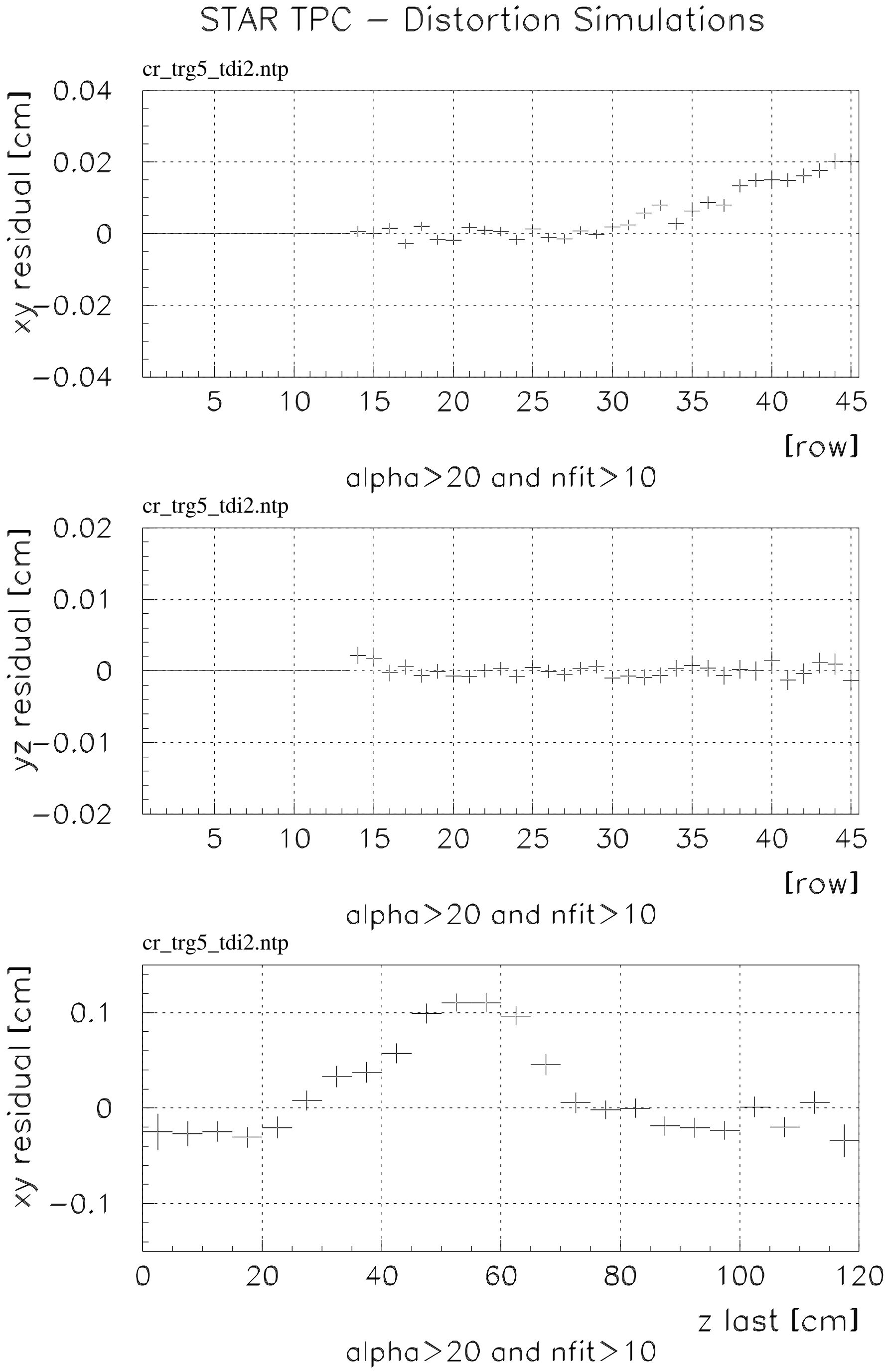

Figure 3: The average xy residual as a function of row (top), the average yz residual as a function of row (middle) and the average xy residual of the last point as a function of z (bottom), for the case of a shorted stripe at $z = 52$ cm. The track fit used rows 14–30.

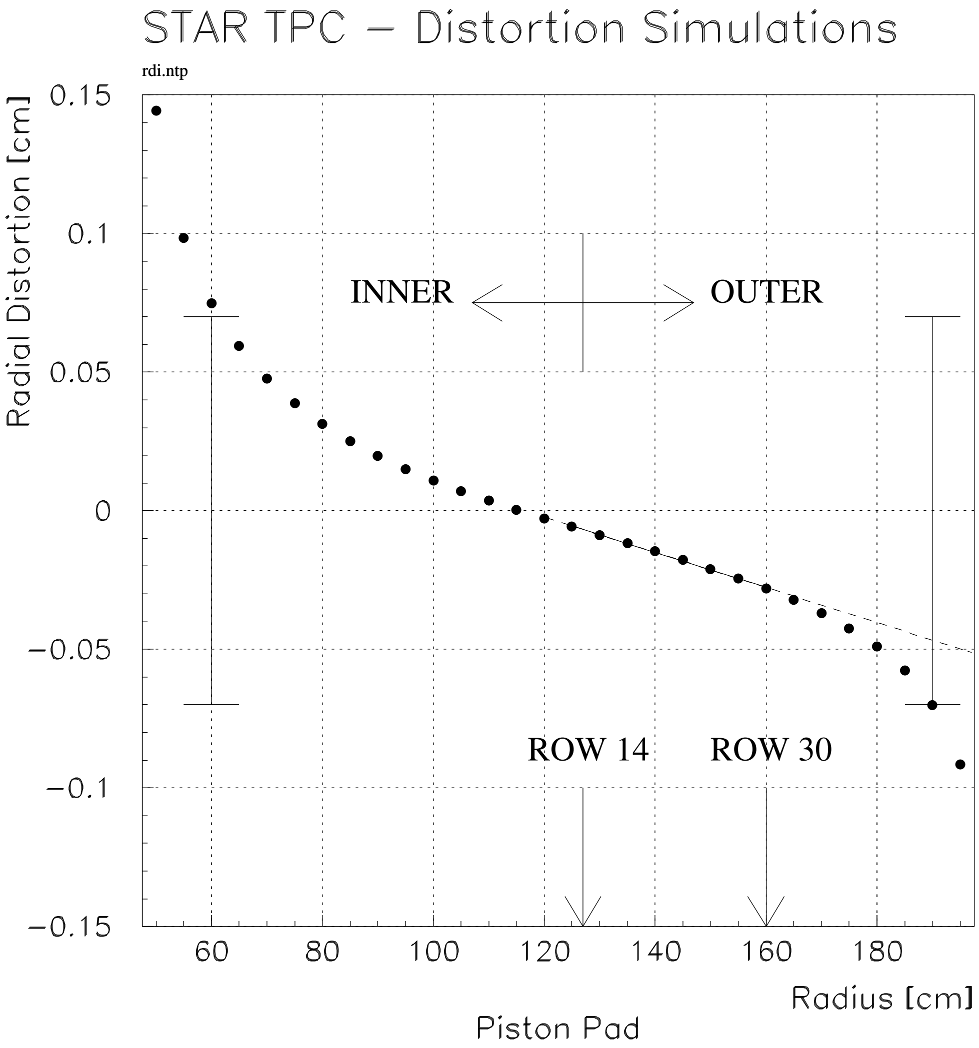

Figure 4: The radial distortion as a function of radius at $z = 0$ cm, for the pad plane plunger effect, with a potential mismatch of $\Delta V/V = 2.5 \times 10^{-4}$.

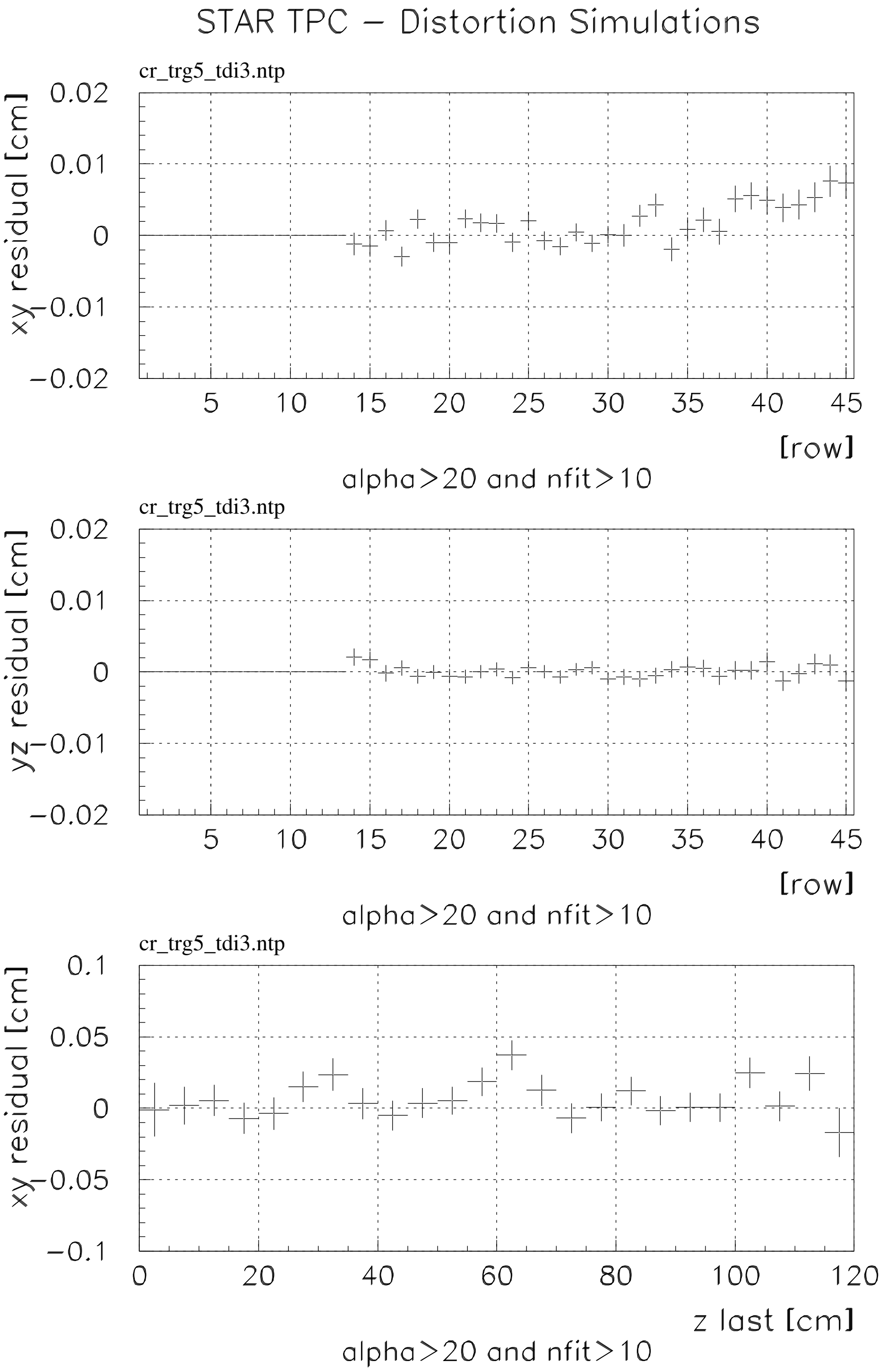

Figure 5: The average xy residual as a function of row (top), the average yz residual as a function of row (middle) and the average xy residual of the last point as a function of z (bottom), for the pad plane plunger effect with a potential mismatch of $\Delta V/V = 2.5\times10^{-4}$. The track fit used rows 14–30.

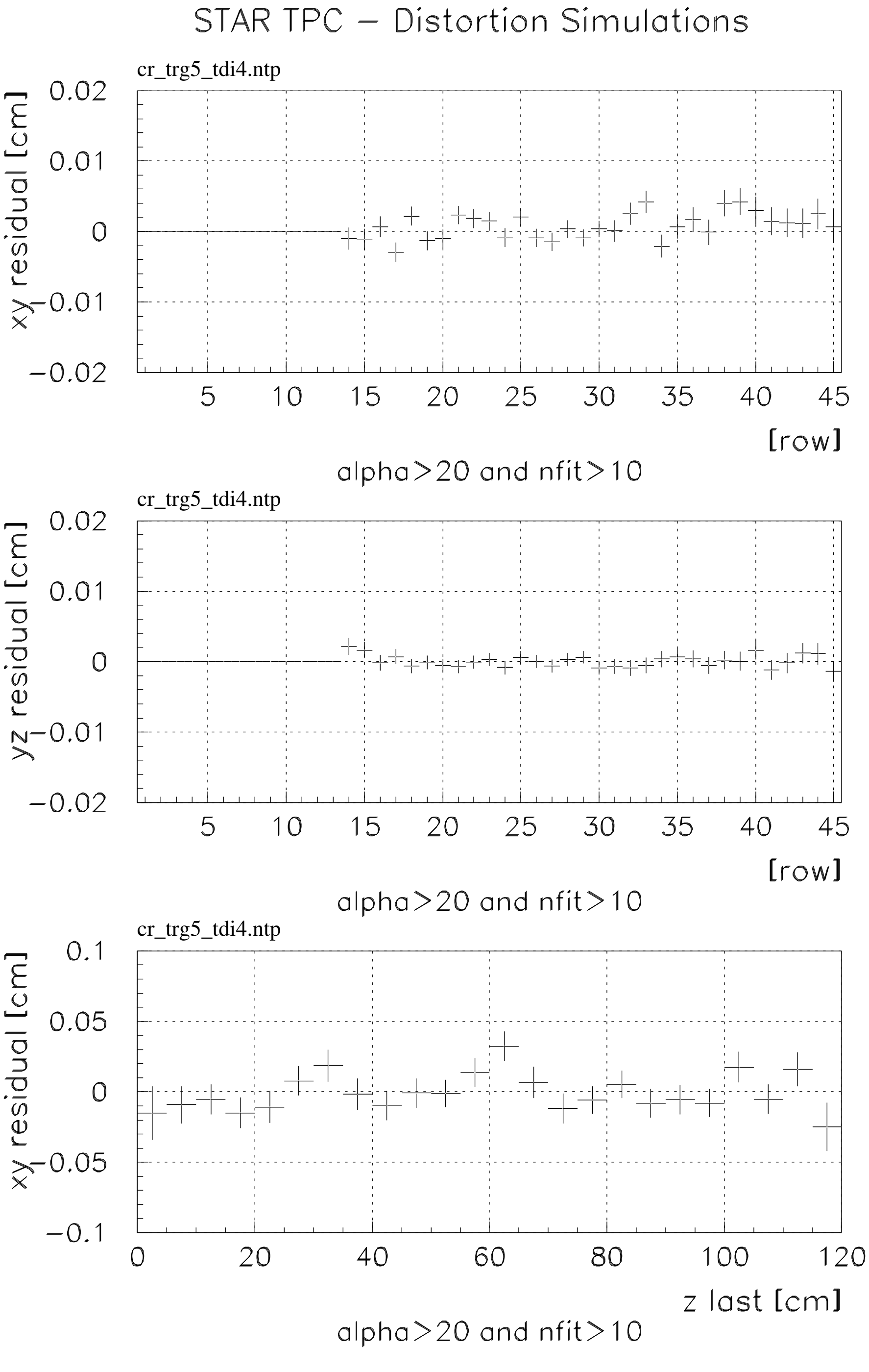

Figure 6: The average xy residual as a function of row (top), the average yz residual as a function of row (middle) and the average xy residual of the last point as a function of z (bottom), for the HV membrane plunger effect with a potential mismatch of $\Delta V/V = 2.5 \times 10^{-4}$. The track fit used rows 14–30.

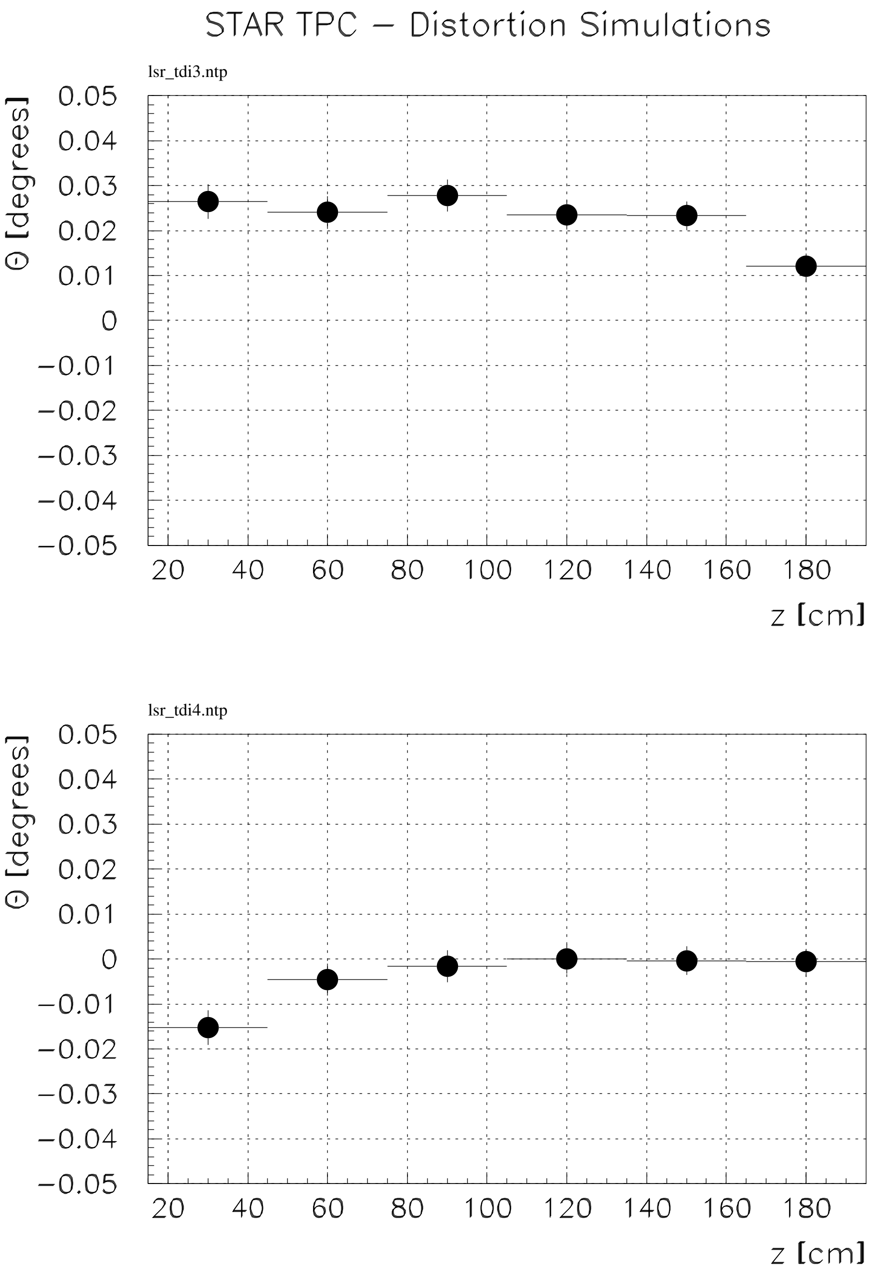

Figure 7: The angle difference between laser tracks from mirrors 3 and 5 as a function of z, for the pad plane plunger effect (top) and the HV plunger effect (bottom). The track fit used all hits in the outer sector only.